Evaluating Trade-offs Between Irrigation Profit and Streamflow Depletion Using a Hydro-Economic Model

Preprint Statement: This is a non-peer-reviewed preprint submitted to EarthArXiv.

The manuscript has not been peer-reviewed or formally published. Subsequent versions may differ slightly. The author retains the right to submit this manuscript to a peer-reviewed journal in the future.

Boyao Tian ¹ *

Andrea Brookfield ¹

Margaret Insley 2

¹Department of Earth and Environmental Sciences, University of Waterloo, 200 University Avenue West, Waterloo, ON, Canada, N2L 3G1.

²Department of Economics, University of Waterloo, 200 University Avenue West, Waterloo, ON, Canada, N2L 3G1.

^{1*} Corresponding Author: boyao.tian@uwaterloo.ca

Abstract

Groundwater overexploitation can reduce flows in connected rivers through streamflow depletion, which threatens ecosystems and downstream users who often rely on these flows for their economic wellbeing. Quantifying groundwater-surface water interactions and their economic trade-offs remains challenging for sustainable water management. This study integrates analytical groundwater and streamflow depletion methods with a farm-level hydro-economic model to evaluate the hydrologic and economic effects of irrigation groundwater pumping illustrated using example applications in confined and unconfined aguifers. The model separates the effect on land value of aguifer storage, streamflow depletion, and direct surface water use, allowing a clearer understanding of how each water source affects economic outcomes. Results from the simulated aquifers show that confined aquifers experience faster and larger streamflow depletion, while unconfined systems exhibit slower and smaller depletion. Distance to the stream and pumping rates are key determinants of depletion, shaping both its timing and magnitude, and they also have distinct effects on land values. The marginal economic value of streamflow depletion is consistently low or negative, suggesting that the water gained through depletion contributes minimally to overall economic returns. These findings highlight the importance of identifying water source contributions, well placement, and regulatory constraints when designing irrigation strategies. Through integrated marginal value and risk analyses, this study offers practical insights for policymakers and water managers to design irrigation strategies that balance economic returns with long-term water resource sustainability.

Keywords: Groundwater Management; Analytical Models; Streamflow Depletion; Groundwater-Surface Water Interaction; Economic Trade-offs; Marginal Value; Irrigation Management

1 Introduction

Groundwater is critical to ecosystems, human health, and industry, including agricultural production. Increasing global food demand, driven by population growth and rising incomes, often met through increased irrigation, poses significant challenges to sustainable groundwater use (Mancosu et al., 2015; Fróna et al., 2019; Hemathilake and Gunathilake, 2022). In many regions, this has led to overexploitation, depleting aquifers and inducing streamflow depletion, where groundwater pumping reduces the water that would naturally support rivers (Barlow and Leake, 2012). This can harm riverside ecosystems, reduce water availability for downstream users, and impact economic activities reliant on streamflow, such as fisheries, mining, and tourism (Palmer et al., 2009; Foglia et al., 2013; Lapides et al., 2022). Additionally, climate change may compound these consequences through altered runoff patterns caused by increased severe weather events (e.g., floods and droughts) and changes in snowmelt timing and volumes (Kienzle et al., 2012; Tanzeeba and Gan, 2012; Zare et al., 2023). Understanding the hydrologic and economic relationships between groundwater pumping for irrigation and streamflow depletion is critical to developing sustainable water management strategies.

Streamflow depletion has been observed worldwide, such as the Wei River Basin in China, High Plains Aquifer and Republican River Basin in the U.S., São Francisco River Basin in Brazil (Kustu et al., 2010; Barlow and Leake, 2012; Ahlfeld et al., 2016; Lucas et al., 2021; Chen et al., 2025). In Canada, it has been observed in regions such as the Assiniboine Delta Aquifer and the Saskatchewan River Basin (Kienzle et al., 2012; Danielescu et al., 2021). However, quantifying streamflow depletion remains challenging due to the complexity of hydrologic systems and the difficulty of distinguishing it from the natural hydrologic variability and human water demands (Zipper et al., 2019, 2022; Lapides et al., 2022).

To evaluate streamflow depletion, both numerical models and analytical methods are

commonly used. Numerical models, such as MODFLOW and FEFLOW are process-based physical models that simulate groundwater flow under complex conditions and can capture streamflow depletion from rivers represented by boundary conditions (Barlow and Leake, 2012; Diersch, 2013; Zipper et al., 2019; U.S. Geological Survey, 2022a). In addition, they have been coupled with surface water flow modules to simulate river dynamics (e.g., MF-OWHM, MIKE SHE), or incorporated into fully integrated hydrologic models such as ParFLOW and HydroGeoSphere (U.S. Geological Survey, 2022b; Aquanty, nd; DHI Group, nd; ParFlow, 2023). However, these models require extensive data, time, and financial investment, making them difficult to develop and promote broadly for addressing water-management problems, particularly among agencies and decision makers who may lack the resources to build or maintain such complex tools. Analytical solutions are less data and computationally intensive compared to numerical models but rely on underlying assumptions and simplifications that limit their applicability (Barlow and Leake, 2012; Zipper et al., 2022). These simplifications typically represent three-dimensional flow systems as one- or two-dimensional systems with idealized boundary conditions, such as completely straight streams and homogeneous aquifer materials (Barlow and Leake, 2012). Several popular analytical solutions for streamflow depletion, including Glover and Balmer (1954), Hunt (1999), and Huang et al. (2018), are designed for different hydrological conditions and data sources, each with its own advantages and limitations which are discussed further in the following section.

Although streamflow depletion has received increasing attention, few studies have quantified its economic trade-offs or examined how it influences farm-level irrigation decisions. This study addresses this gap by extending the hydro-economic framework developed by Tian et al. (2025a,b) to explicitly incorporate groundwater-surface water interactions and the economic consequences of streamflow depletion. The enhanced model provides a tool to evaluate how depletion dynamics affect irrigation strategies, balancing economic viability

with long-term resource sustainability. The outcomes contribute to preserving ecosystem function and agricultural profitability, supporting sustainable water resource management, and helping policymakers and farmers align economic incentives with environmental conservation goals.

2 Methods

This paper builds on a hydro-economic model developed by Tian et al. (2025a), where detailed methodology can be found. The hydrologic model includes stochastic precipitation based on Richardson (1981), groundwater drawdown using the Cooper Jr and Jacob (1946) method, evapotranspiration estimated using the FAO Penman-Monteith method (Allen et al., 1998), and yield model modified from Martin et al. (2010) and Klocke (2011). The economic model includes a stochastic crop price model following a Mean Reversion process, along with cost functions to estimate annual cash flows and discounted land values.

A key highlight of this integrated model in Tian et al. (2025a,b) is the use of Conditional Value-at-Risk (CVaR) to assess economic risks associated with groundwater irrigation. CVaR focuses on the tail of the probability distribution, making it a more robust risk metric compared to traditional methods such as Value-at-Risk (VaR) (Rockafellar et al., 2000; Rockafellar and Uryasev, 2002; Sarykalin et al., 2008). In this study, we use CVaR to represent the average of the worst 5% of land values, providing a measure of a farm's potential downside value compared with the mean. By capturing extreme low-income scenarios, CVaR enables a detailed assessment of the risks associated with irrigation decisions and strengthens the robustness of the analysis.

The following section focuses only on the streamflow depletion component and presents the equations that differ from previous studies of Tian et al. (2025a,b).

2.1 Conceptual Model

The model developed for this work can capture four scenarios of groundwater-surface water interactions. In Figure 1a and c, the water table is hydraulically disconnected from the stream, meaning groundwater pumping has no impact on streamflow. These cases were examined in previous studies (Tian et al., 2025a,b). In this paper, we focus on the connected cases (Figure 1b and d), where groundwater pumping induces streamflow depletion. As pumping starts, the cone of depression expands and eventually reaches the river boundary. At that point, the stream acts as a recharge source, and stream water is drawn into the pumping well. Consequently, the cone of depression on the stream side stabilizes, and groundwater drawdown is determined by the specified boundary conditions discussed in Section 2.3.1.

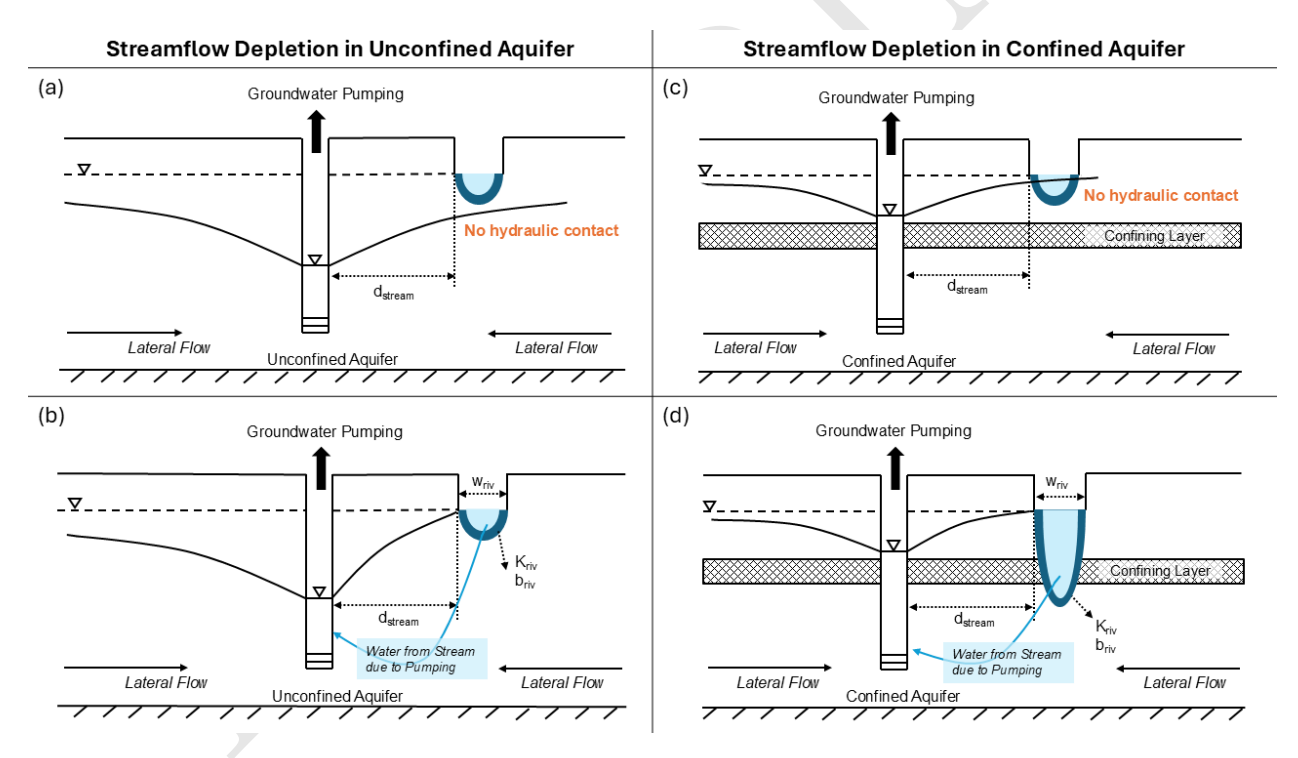


Figure 1: Conceptual models of streamflow depletion: (a) unconfined aquifer, no hydraulic contact; (b) unconfined aquifer, streamflow depletion occurs; (c) confined aquifer, no hydraulic contact; (d) confined aquifer, streamflow depletion occurs.

2.2 Quantifying the Effects of Streamflow Depletion

The analytical models used for streamflow depletion in this study assume a homogeneous, isotropic aquifer of infinite extent, with recharge unaffected by pumping and only lateral groundwater flow considered (vertical flow, aside from recharge, is neglected). The stream is represented as a straight, infinitely long channel with constant stage and no streambank storage (Huggins et al., 2018). While these assumptions simplify real-world conditions, they provide reasonable approximations for identifying key hydrologic trends and economic tradeoffs, making the approach suitable for evaluating groundwater-surface water interactions at a conceptual level. In addition, analytical solutions provide clearer hydrologic intuition compared to more complex numerical models, making it easier to understand how groundwater and streamflow depletion respond to pumping decisions. Two analytical solutions are explored in this work: Glover's method (Glover and Balmer, 1954) and Hunt's method (Hunt, 1999); both methods are applicable to confined and unconfined systems.

2.2.1 Glover's Method

Glover's method (Glover and Balmer, 1954) is a simple analytical approach that assumes a fully penetrating stream with no resistance to flow across the streambed (Figure 2a):

$$\frac{Q_{sdG}}{Q_{gw}} = \operatorname{erfc}\left(\sqrt{\frac{Sd_{\text{stream}}^2}{4T_{\text{aquifer}}t_s}}\right) \tag{1}$$

Where Q_{sdG} is streamflow depletion rate from Glover's method $[L^3T^{-1}]$, Q_{gw} is groundwater pumping rate $[L^3T^{-1}]$; erfc is complementary error function; S is storage coefficient (specific yield for unconfined systems or storativity for confined systems) [-]; d_{stream} is the distance from pumping well to stream [L]; T_{aquifer} is transmissivity $[L^2T^{-1}]$, given by $T_{\text{aquifer}} = Kb$, where K is the hydraulic conductivity $[LT^{-1}]$, and b is the aquifer thickness [L]; t_s is the time start of pumping [T].

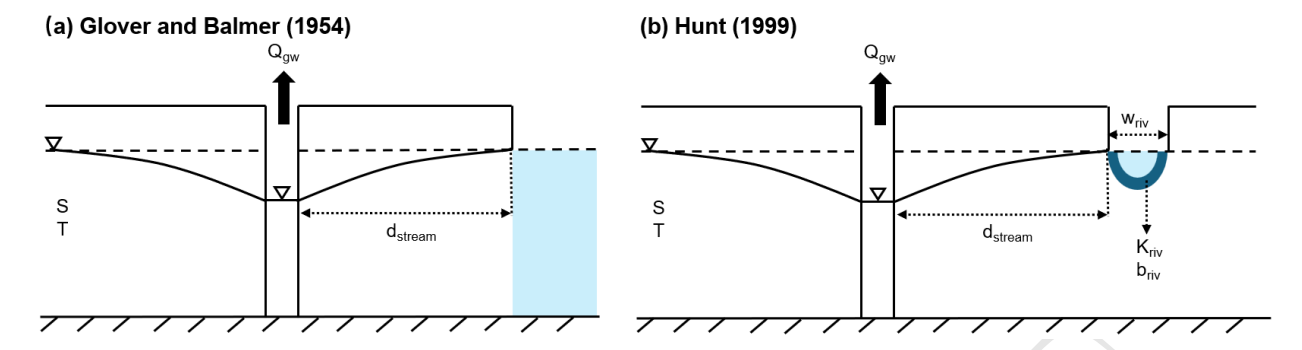


Figure 2: Illustration of two analytical models: (a) Glover's method; (b) Hunt's method.

2.2.2 Hunt's Method

Hunt (1999) method builds from Glover's method and accounts for a partially penetrating stream and incorporates the effect of a partially clogging streambed, making it more representative of many real-world conditions (Figure 2b). To distinguish between the two methods, we use Q_{sdH} to represent the estimated streamflow depletion based on Hunt's method. The corresponding equations are:

$$\frac{Q_{sdH}}{Q_{gw}} = \operatorname{erfc}\left(\sqrt{\frac{Sd_{\text{stream}}^2}{4T_{\text{aquifer}}t_s}}\right) - \exp\left(\frac{\lambda^2 t_s}{4ST_{\text{aquifer}}} + \frac{\lambda d_{\text{stream}}}{2T_{\text{aquifer}}}\right) \operatorname{erfc}\left(\sqrt{\frac{\lambda^2 t_s}{4ST_{\text{aquifer}}}} + \sqrt{\frac{Sd_{\text{stream}}^2}{4T_{\text{aquifer}}t_s}}\right)
(2)$$

$$\lambda = \frac{w_{\text{riv}}K_{\text{riv}}}{b_{\text{riv}}}$$
(3)

Where λ is streambed conductance $[LT^{-1}]$; w_{riv} is river width [L], K_{riv} is streambed hydraulic conductivity $[LT^{-1}]$, b_{riv} is streambed thickness [L]. Because streambed conductance tends to be lower than the conductance of the subsurface media, this method typically predicts less severe depletion than Glover's method during pumping periods shorter than the time needed to reach a new steady state (Huggins et al., 2018). We compare and validate our depletion results with STRMDEPL08 from U.S. Geological Survey (2013) in Supplementary A.

2.3 Quantifying the Effects on Water Level

This work builds on the model presented in Tian et al. (2025a) which estimates changes in groundwater levels based on Cooper Jr and Jacob (1946) drawdown from pumping. In this paper, we include boundary conditions to account for the effect of a hydraulically connected stream on groundwater levels. The other model components remain unchanged, so we do not repeat the detailed discussion of the original model here.

2.3.1 Boundary Conditions

Streams in hydraulic connection with the aquifer can be represented as constant head boundaries where the hydraulic head remains fixed (also known as recharge boundaries) (Ferris et al., 1962), as shown in Figure 3. The orange dashed line is the initial drawdown and cone of depression without the presence of a stream. When the stream is present, it can be included mathematically as an infinite recharge source using superposition (Ferris et al., 1962). To simulate this, an imaginary recharge well is placed at an equal distance from the stream but on the opposite side of the real pumping well (Ferris et al., 1962). According to the principle of superposition, the actual drawdown at the pumping well is represented by the sum of the orange dashed line and the green dotted line, resulting in the blue solid line where the drawdown is exactly zero at the constant-head boundary.

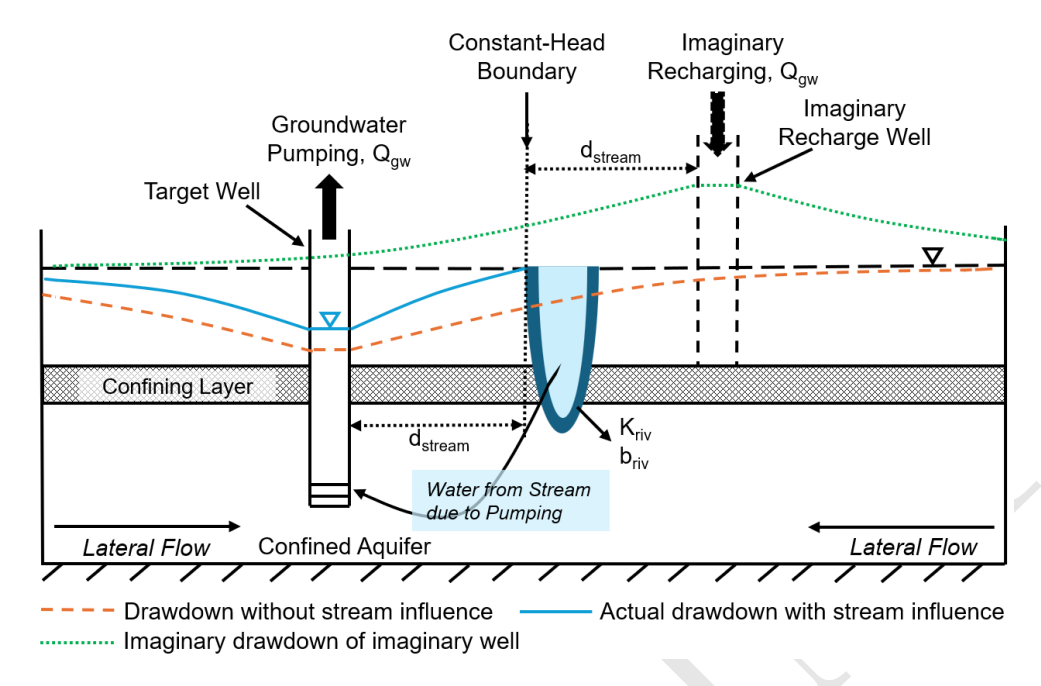


Figure 3: Illustration of the representation of streams as constant-head boundary conditions in drawdown calculations (modified from Ferris et al. (1962)).

The mathematical process for calculating drawdown is outlined as follows. Regular drawdown (S_{target} [L]) in the target well from an infinite aquifer from Cooper Jr and Jacob (1946):

$$S_{\text{target}} = \frac{Q_{gw}}{4\pi T_{\text{aquifer}}} \left[-0.5772 - \ln\left(\frac{r_w^2 S}{4T_{\text{aquifer}} t_p}\right) \right] \tag{4}$$

where r_w is the effective radius of the well [L]; t_p is the duration of pumping [T].

Drawdown in the imaged recharge well (S_{recharge} [L]) (Ferris et al., 1962):

$$S_{\text{recharge}} = \frac{-Q_{gw}}{4\pi T_{\text{aquifer}}} \left[-0.5772 - \ln\left(\frac{(2d_{\text{stream}})^2 S}{4T_{\text{aquifer}} t_p}\right) \right]$$
 (5)

Corrected drawdown (S_{bounded} [L]) based on superposition principle (Ferris et al., 1962):

$$S_{\text{bounded}} = S_{\text{target}} + S_{\text{recharge}}$$
 (6)

Extra drawdown (S_{eff} [L]) due to well efficiency (Eff [-]) (Brookfield, 2016):

$$S_{\text{eff}} = \left(\frac{100}{\text{Eff}} - 1\right) S_{\text{bounded}} \tag{7}$$

Total drawdown (S_{total} [L]) in the target well:

$$S_{\text{total}} = S_{\text{bounded}} + S_{\text{eff}}$$
 (8)

All drawdown values used in the following sections are total drawdown, including boundary conditions and well-efficiency corrections.

2.4 Economic Analysis

To assess economic value, this study applies the hydro-economic model to estimate land values. Land value is defined as the expected value of the discounted sum of net cash flows from crop harvesting over a specified number of years, and given a particular strategy for irrigation decisions and groundwater withdrawals. Here, land value is decomposed into five components: (1) benefits from surface water irrigation, (2) benefits from groundwater irrigation, (3) benefits from streamflow depletion, (4) benefits from precipitation (non-irrigated water), and (5) fixed costs such as land and machinery. For the first three components, net returns are calculated as crop revenue minus variable costs (e.g., pumping, delivery fees, fertilizer, and other yield-related expenses). Net returns from precipitation depend only on the portion of crop yield supported by rainfall, without any irrigation-related costs. The fixed-cost component represents annual costs for land and machinery that do not vary with yield but recur each year. We discount all annual values to the present and sum them over the planning horizon to obtain each component's contribution to land value. The percentages of these components sum to one.

Notably, groundwater irrigation includes only water pumped directly from the aquifer, while streamflow depletion is treated separately because it represents stream water derived through the pumping well. Surface water irrigation represents water directly diverted from the stream. Because all components are calculated from the same underlying annual net returns, their discounted contributions add up to the total land value. This breakdown allows readers to see clearly how each water source and the hydrologic consequences of pumping contributes to economic outcomes.

Additionally, this study estimates the marginal values of streamflow depletion (i.e., the part of water derived from stream through pumping well), following the approach of Samarawickrema and Kulshreshtha (2009). These marginal values are calculated for each year, since the economic contribution of streamflow depletion changes over time as groundwater levels, pumping costs, and crop yields evolve.

For a given year, the marginal value of product from streamflow depletion (MVP_{SD}) is defined as the marginal product (MP_{SD}) multiplied by the crop price (P_{crop}). The MP_{SD} is the increase in crop yield (Δ Yield) from a unit increase in streamflow depletion (ΔQ_{sd}). The marginal cost of streamflow depletion (MC_{SD}) includes both the additional pumping energy required for a unit increase in streamflow depletion, measured as the change in energy use (Δ Energy) multiplied by the energy price (C_e), and the associated yield-related production costs (C_y). The marginal net benefit (MNB_{SD}) represents the net economic gain (or loss) to the farmer from using one more unit of streamflow-depleted water in that year.

$$MVP_{SD} = MP_{SD} \times P_{crop}$$
 (9)

$$MP_{SD} = \frac{\Delta Yield}{\Delta Q_{sd}}$$
 (10)

$$MC_{SD} = \Delta Energy \times C_e + \Delta Yield \times C_y$$
 (11)

$$MNB_{SD} = MVP_{SD} - MC_{SD}$$
 (12)

Analyzing marginal benefits and costs at the yearly scale provides intuition about shortterm decision-making. In practice, farmers may adjust pumping within a season based on immediate returns, and annual marginal values help illustrate how streamflow depletion affects profitability through its influence on yield, pumping effort, and input costs.

3 Study Site

This integrated study is applied to a farm site in the Saskatchewan River Basin, the target irrigation well is located near Arrowwood Village, Vulcan County, southern Alberta. The site pumps groundwater from the Buried Valleys Aquifer System (confined aquifer) and uses surface water from the Bow River (Cummings et al., 2012; GIN, 2021). Detailed information and the target well map can be found in Tian et al. (2025b).

The Saskatchewan River Basin (SRB) in western Canada has a drainage area over $400,000 \, km^2$, spanning parts of Alberta, Saskatchewan, and Manitoba, which is a crucial agricultural region, producing 75% of Canada's irrigated crops (Pomeroy et al., 2005; Axelson, 2007; Gober and Wheater, 2014). Future climate change may intensify streamflow depletion by altering the timing and magnitude of runoff, particularly through earlier snowmelt and increased drought frequency (Comeau et al., 2009; Moore et al., 2009; Marshall et al., 2011; Bonsal et al., 2013).

Although previous studies in the SRB have explored streamflow trends and river vulnerability (Tanzeeba and Gan, 2012; Keshavarz et al., 2021; Hamdi and Goïta, 2023), fewer have focused specifically on depletion driven by groundwater pumping. Given the region's dependence on both groundwater and surface water for irrigation, this study highlights the importance of capturing stream-aquifer interactions in hydro-economic modeling to support sustainable water use in the basin.

4 Results

This section presents streamflow depletion analysis for the SRB farm site, followed by economic assessments. All simulations are conducted over a 20-year time horizon unless stated otherwise. Monte Carlo simulations with 10,000 iterations are applied, and streamflow depletion is calculated using Hunt's method (Equations 2 and 3). Other simulation settings and parameters are consistent with Tian et al. (2025b). A comparison of the two analytical methods used to estimate streamflow depletion, with parameter sensitivity tests, is provided in Supplementary B.

4.1 Streamflow Depletion in the SRB Farm Site

We selected 16 wells near the SRB farm site, with distances to the Bow River ranging from 250 m for the closest well to approximately 5000 m for the furthest well (Figure 4). Assuming consistent hydrologic conditions, we focused on the impacts of distance and time on streamflow depletion. Figure 5 shows the fraction of streamflow depletion at different distances over 10, 20, and 50 years. The results clearly indicate that closer wells cause greater depletion, while the differences across time scales are relatively small. When the distance exceeds 4000 m, the changes in streamflow depletion fractions become insignificant. However, as the time scale extends, more depletion occurs overall.

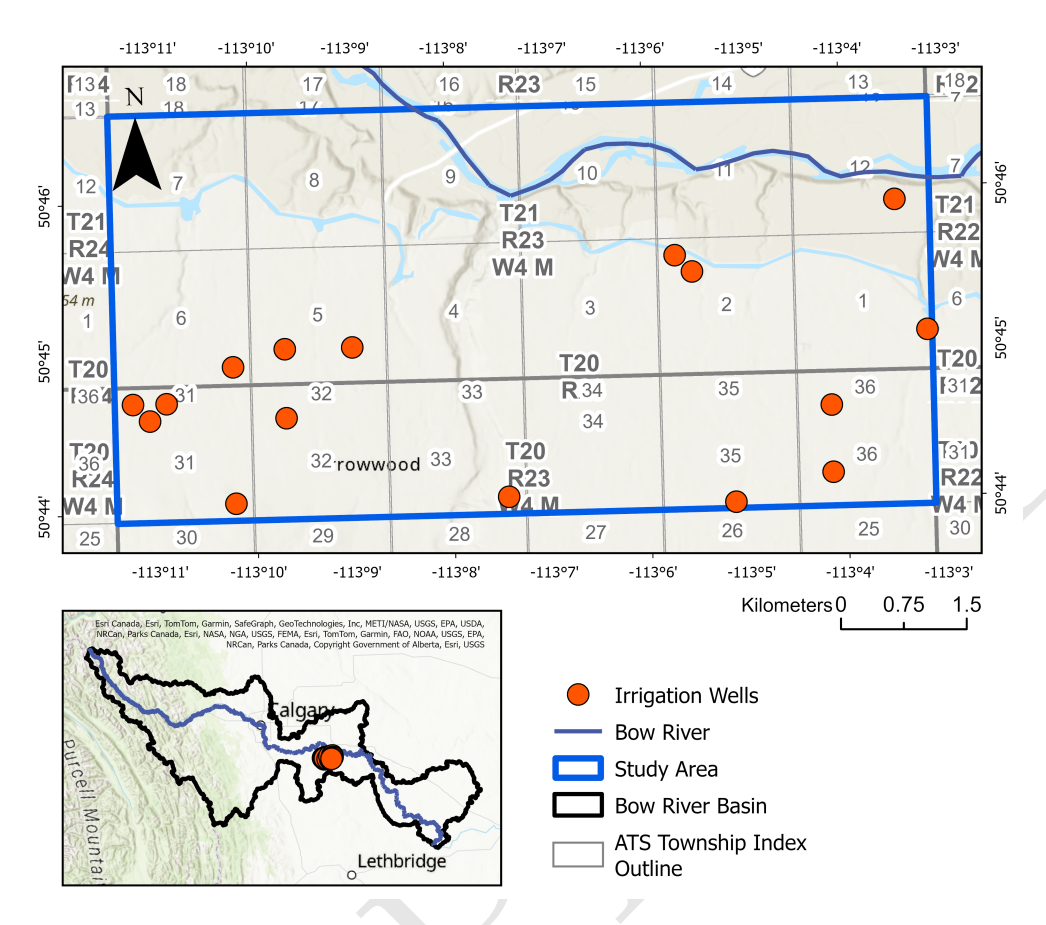


Figure 4: Maps of tested wells, data is from AFCC (2013).

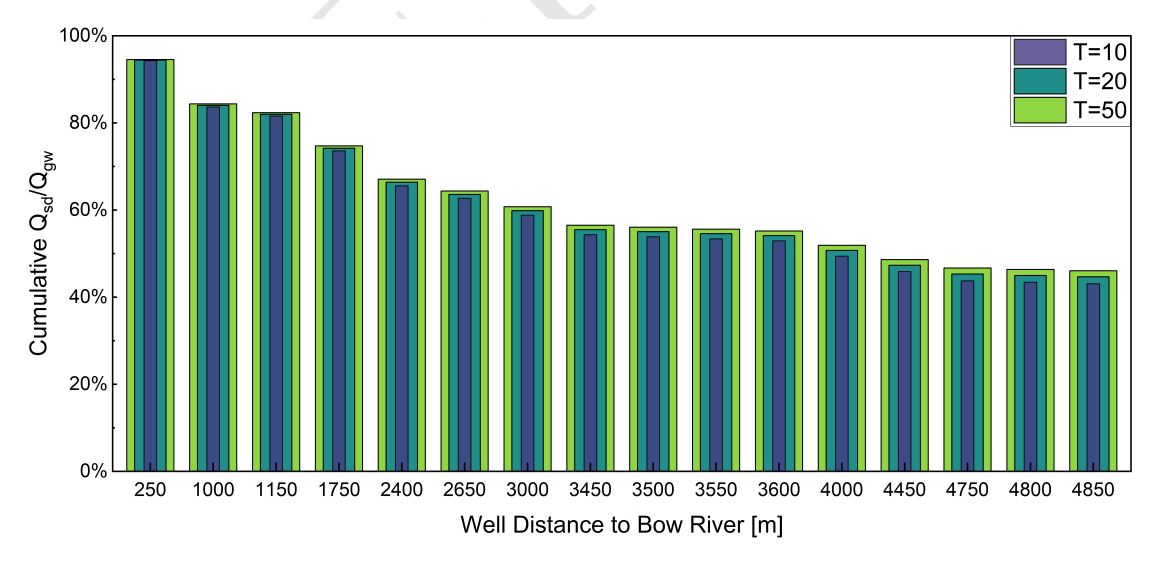


Figure 5: Fraction of streamflow depletion under different distances for different time scales.

To illustrate the hydrologic effects of streamflow depletion, Figure 6 compares ground-

water level changes for a well located 500 m from the stream with a hypothetical well under identical conditions but without a nearby stream. The stream serves as a recharge source, so wells that induce streamflow show shallower water depths. In contrast, the no-stream case relies only on aquifer storage, leading to larger drawdown. The average streamflow depletion rate remains relatively stable because the Monte Carlo simulations average out variations across multiple realizations. This comparison shows the importance of accounting for groundwater-surface water interactions, as water level differences influence aquifer longevity and reveal the adverse impacts on streams. Additional analysis on land value outcomes is provided in the following sections.

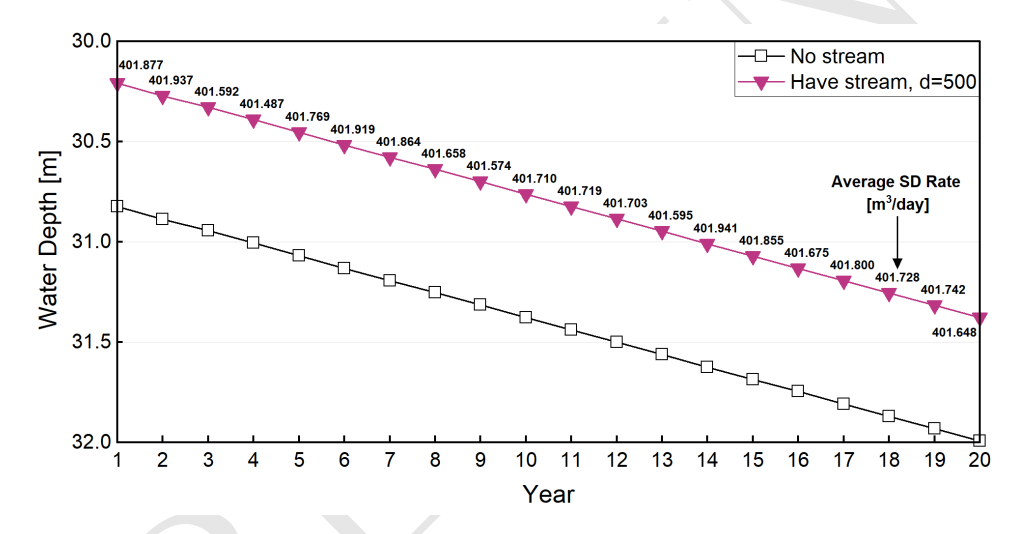


Figure 6: Water depth changes for streamflow depletion case and no-stream case, with labelled average streamflow depletion rate.

4.2 Economic Analysis

In this section, we apply the hydro-economic model to estimate land values, evaluate the contributions of different water sources, and use marginal values to assess the short term economic returns of water derived from streamflow depletion. The confined aquifer case is represented by the SRB site, while an unconfined case is illustrated through a hypothetical site to highlight key differences.

4.2.1 Confined Aquifers

We first conduct an economic analysis for a well located close to the stream ($d_{\text{stream}} = 500$ m), where drawdown is heavily influenced by the river (Figure 7 (a1–c1)); then evaluate a pumping well located further from the stream ($d_{\text{stream}} = 4500$ m), where boundary condition does not occur (i.e., using regular drawdown in Equation 4 with well efficiency corrections) (Figure 7 (a2–c2)). Land value is shown in Figure 7 for different regulatory pumping limits, assuming the pumping limit is held constant over the full 20 year horizon of the analysis.

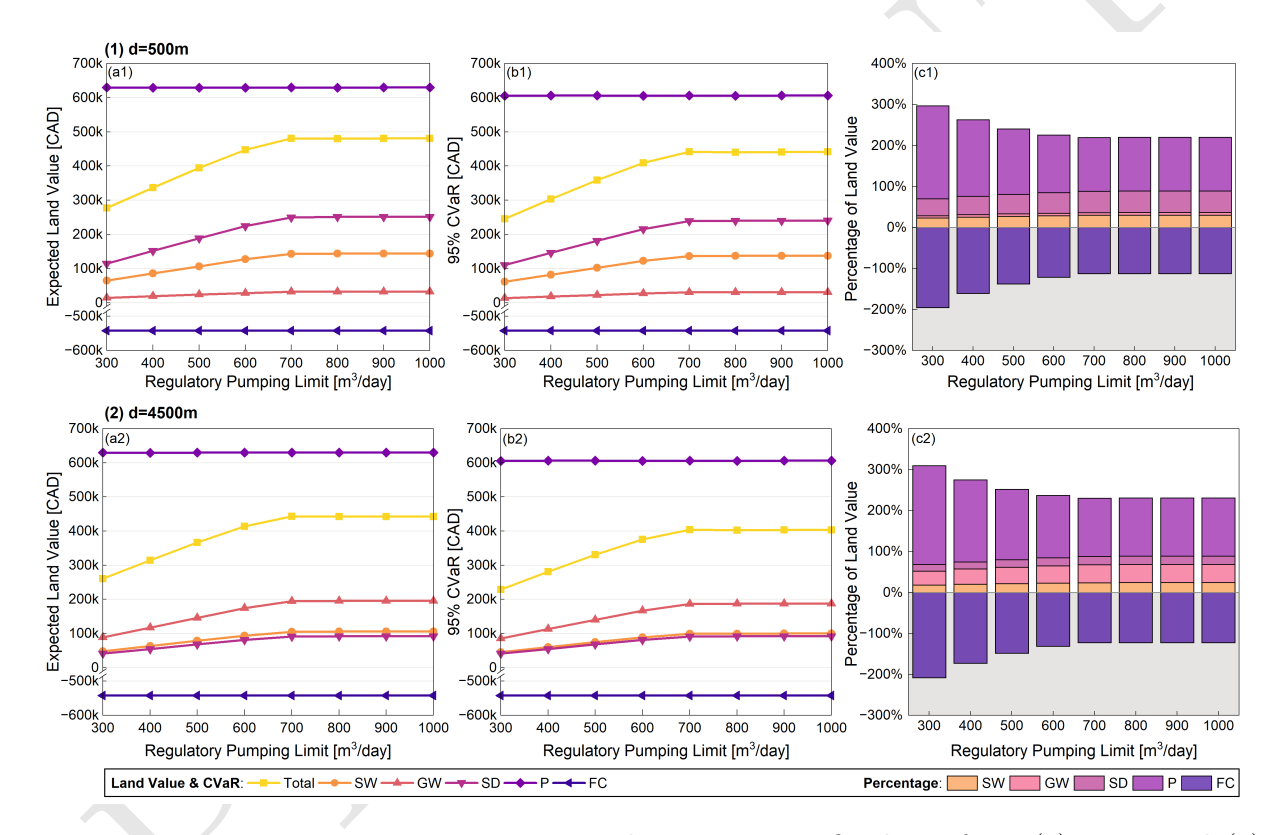


Figure 7: Economic outcomes at two stream distances in confined aquifers: (1) 500m and (2) 4500m. Subplots: (a) expected land value, (b) 95% CVaR, (c) percentage contributions (SW = surface water; GW = groundwater; SD = streamflow depletion; P = precipitation; FC = fixed costs).

In Figure 7, total expected land value (yellow line) increases as pumping limits are relaxed, peaking at ~700 m³/day. At this point, the average expected land value is around \$480k (Figure 7a1), while the corresponding 95% CVaR is about \$440k (Figure 7b1), indi-

cating that in the worst 5% of cases, the average land value would be \$440k. Similar annual precipitation contributes to stable land values across irrigation scenarios. As expected, precipitation's relative contribution decreases as pumping increases (Figure 7c). Fixed costs account for a large percentage of total land value, especially under deficit irrigations. For the closer well (Figure 7 (a1–c1)), streamflow depletion dominates the irrigation components, a significant portion of the pumped water is derived from the stream rather than the aquifer. Direct surface water is the second-largest contributor, followed by groundwater.

For the farther well (Figure 7 (a2–c2)), groundwater becomes the largest contributor, streamflow depletion has less impact on the land values and creates similar values to direct surface water. Total land value also peaks at a pumping limit of ~700 m³/day, reaching around \$440k (Figure 7a2), with a corresponding 95% CVaR of about \$400k (Figure 7b2). Total land value of the farther well is ~8% lower than closer well's, partly due to higher surface water delivery fees. CVaR is ~10% lower than closer well's, suggesting that the worst-case outcomes are more severe and the system is more exposed to downside risk.

In addition to evaluating different regulatory pumping limits, we also test two groups of irrigation strategies (Table 1). Group A: different irrigation fraction (constant and two-stage time-varying), where the irrigation fraction represents the percentage of crop water demand that farmers choose to apply (e.g., $\beta=1$ indicates full irrigation; $\beta=0.9$ applies 90% of crop water demand). This allows us to evaluate whether farmers benefit more from maintaining a consistent irrigation level or adjusting irrigation intensity across the growing season. Group B: different groundwater-surface water ratio (constant over time), representing decisions about how much irrigation water is drawn from groundwater versus surface water (e.g., 0.8 GW-0.2 SW means 80% groundwater and 20% surface water). These choices influence pumping costs, delivery fees, and streamflow depletion. Farmers may adjust both the irrigation fraction (Group A) and the water-source ratio (Group B) depending on their water rights, available allocations, and cost considerations. Together, these strategies cap-

ture a realistic range of farmer decision-making and allow us to assess how different irrigation practices influence economic returns and groundwater-surface water interactions.

Table 1: Irrigation strategies.

Group	Irrigation Fraction (β)		
	$t \leq T/2$	t > T/2	
A1		1	
A2		0.95	
A3		0.9	
A4	1	0.9	
A5	0.95	0.9	
A6	0.9	1	
A7	0.9	0.95	
	Groundwater-Surface Water Ratios		
	GW	SW	
B1	1	0	
B2	0.8	0.2	
В3	0.67	0.33	
B4	0.5	0.5	
B5	0.33	0.67	
B6	0.2	0.8	
B7	0	1	

In Figure 8 (a1–c1), full irrigation (strategy A1, irrigation reaches full crop water demand) yields the highest land value and CVaR, but also the greatest standard deviation and streamflow depletion. The 90% irrigation case (A3) produces the lowest outcomes, while other strategies show similar patterns. In Figure 8 (a2–c2), 100% surface water use results in the highest land value and CVaR, the lowest depletion, and a moderate standard deviation, appearing most favorable. However, this does not imply reduced total water use; larger surface water ratios reflect a smaller portion of induced streamflow depletion, as more water is directly diverted from the stream. This analysis does not account for potential negative impacts or temporal variability in surface water availability.

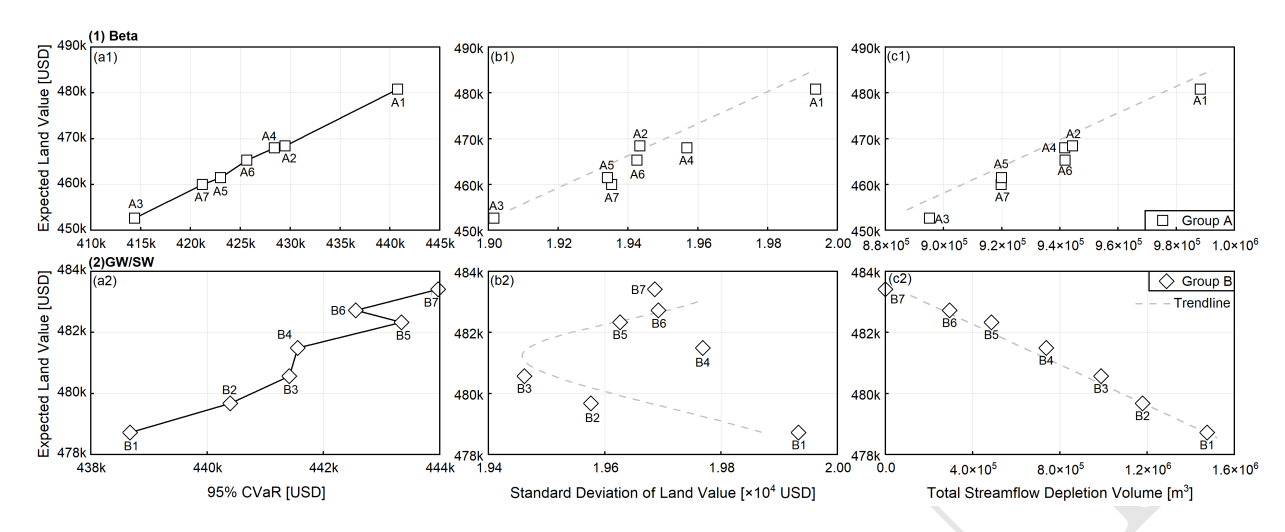


Figure 8: Expected land value vs. risk metrics (a and b), and streamflow depletion (c) under different irrigation strategies: (a1–c1) Group A: irrigation fraction (β); (a2–c2) Group B: groundwater-surface water ratios (GW/SW).

We also examined the relationship between expected discounted cumulative cash flows and groundwater levels (Figure 9), noting that all cash flows are discounted to account for the time value of money. Overall, cumulative cash flows increase as groundwater levels decline, which is expected as the water extracted is used to increase crop yield. Scenarios with streamflow depletion produce slightly higher land values (\$480.82k) than those without access to a stream (\$480.69k), as the stream acts as a recharge source, maintaining shallower water levels and reducing pumping costs. The figure also isolates the portion of cash flows directly attributable to streamflow depletion, which follows a similar increasing trend with increased water depth.

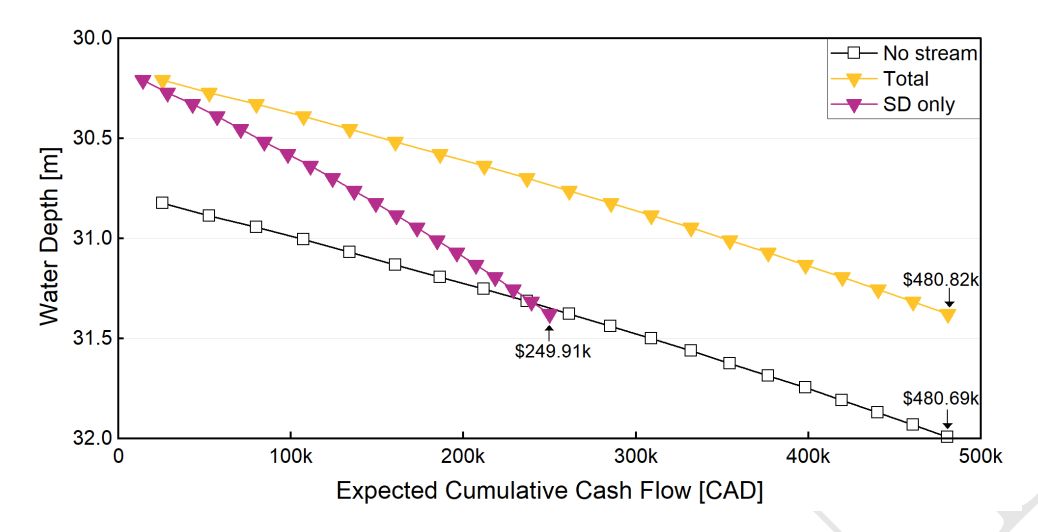


Figure 9: Expected cumulative cash flows and water depth: Total = from all components when a stream is present; SD = from streamflow depletion component only; No stream = from all components but no stream.

4.2.2 Unconfined Aquifers

This section applies the model to an unconfined aquifer. All parameters remain the same as in section 4.2.1, except for using specific yield instead of storage coefficient and accounting for changing aquifer thickness each year. This example demonstrates that the model is adaptable to both confined and unconfined systems, supporting its broader use across diverse hydrogeologic settings. Additional comparisons and detailed parameter descriptions for the confined and unconfined cases are provided in Supplementary B.

For unconfined aquifers (Figure 10), total land value, non-irrigated value (precipitation derived yield), and fixed costs show no significant changes compared to the confined case, and are therefore not repeated here. In terms of irrigation contributions, groundwater provides the largest share, followed by direct surface water and then streamflow depletion, which is opposite to the confined case, where streamflow depletion dominated. This contrast arises because streamflow depletion develops more slowly and to a lesser extent in unconfined systems, where the higher storage capacity and delayed hydraulic response buffer the connection between groundwater pumping and streamflow; this result can also be confirmed in Figure

B3. These results highlight the importance of identifying water source contributions before designing site-specific irrigation strategies to avoid ineffective or unsustainable irrigation policies.

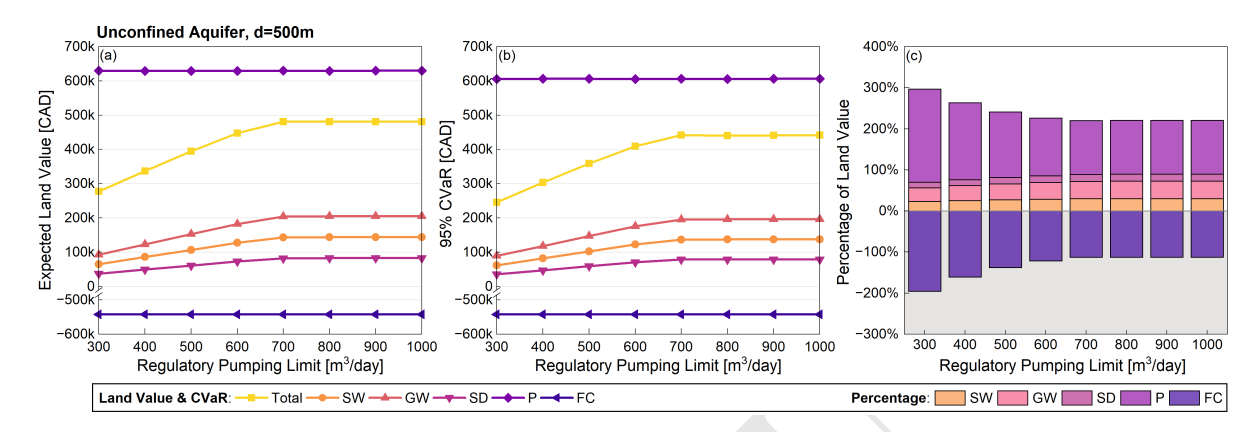


Figure 10: Economic outcomes in unconfined aquifers, d=500m: (a) expected land value, (b) 95% CVaR, (c) percentage contributions (SW = surface water; GW = groundwater; SD = streamflow depletion; P = precipitation; FC = fixed costs).

4.2.3 Marginal Values

To further evaluate the economic implications of streamflow depletion, we analyzed the marginal value product (MVP), marginal cost (MC), and marginal net benefit (MNB) of streamflow depletion across different simulation years (5th, 10th, and 20th year) without discounting. To enable this analysis, irrigation water use is fixed at 400 m³/day directly from surface water, while groundwater pumping varies from 0 to 1000 m³/day in steps of 10. Because the streamflow depletion rate depends only on groundwater pumping (Equation 2), each 10 m³/day increase in pumping corresponds to an 8.9 m³/day increase in depletion in this example. We refer to this 8.9 m³/day increment as "per unit SD" in the subsequent analysis and figures.

In Figure 11a, the MVP represents the crop revenue associated with using one more unit of streamflow depletion in a particular year. MVP remains relatively stable (~40–48 CAD) until the depletion rate reaches about 600 m³/day, after which it declines as yield gains

flatten under the yield response. Figure 11b shows the corresponding MC, including both pumping energy and harvest costs related to crop yield. MC values start ~60–80 CAD but decrease sharply beyond 600 m³/day as yield-related costs diminish (additional irrigation no longer increases crop yield). The resulting MNB in Figure 11c remains negative across all years and depletion levels, indicating that depletion costs consistently exceed direct economic gains. MNB becomes less negative at higher depletion rates, reflecting diminishing marginal returns. Earlier years (e.g., year 5) show smaller losses due to shallower drawdown and lower pumping costs, while by year 20, deeper drawdown drives larger net losses despite stable marginal yields.

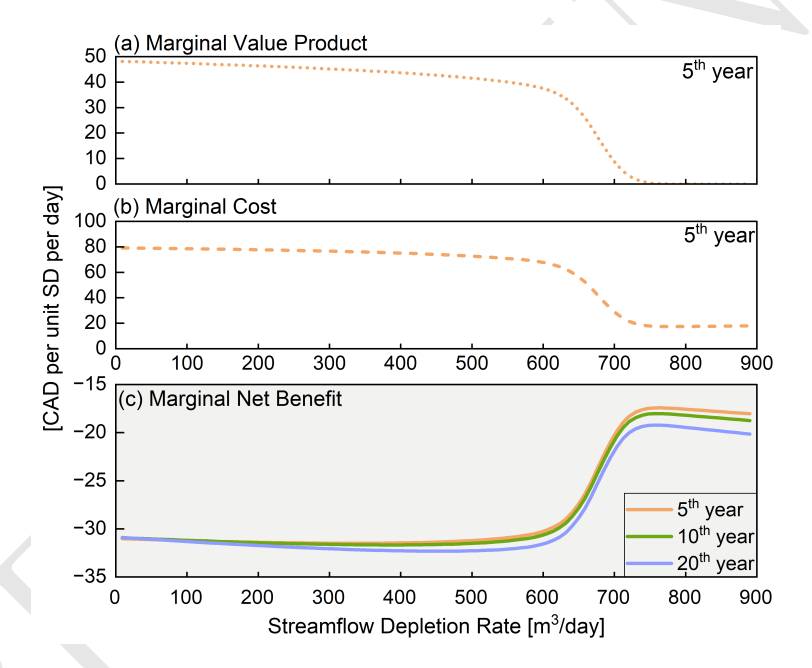


Figure 11: Marginal values of streamflow depletion for the 5^{th} , 10^{th} , and 20^{th} years. (a) Marginal value product, (b) Marginal cost, and (c) Marginal net benefit.

5 Discussion

We use Glover's and Hunt's analytical methods to estimate streamflow depletion from 16 irrigation wells near the Bow River in the SRB. While Glover's method predicts higher depletion due to its assumption of a fully penetrating stream, Hunt's more realistic approach includes streambed resistance. Depletion decreases with distance from the stream and exhibits a time lag due to delayed hydraulic connection. Closer wells cause immediate depletion, while distant ones draw initially from storage. These results align with previous research, reinforcing the importance of spatial and temporal dynamics in managing groundwater-surface water interactions.

By applying the hydro-economic model, this study quantifies land values while explicitly incorporating streamflow depletion and boundary conditions. When land values are separated into different components, non-irrigated yield contributes most to overall land value for the SRB example (Figure 7), highlighting the importance of baseline productivity. Comparing wells in confined aquifer at different distances from the stream reveals strong spatial contrasts: near-stream wells derive most of their irrigation returns from streamflow depletion, whereas distant wells rely primarily on aquifer storage, making groundwater the dominant contributor to land value.

Land value analysis in unconfined aquifers shows contrasting results: even wells near the stream rely more on aquifer storage than on streamflow depletion (Figure 10), reflecting the slower and smaller response of unconfined systems. This highlights the need to consider both economic returns and aquifer characteristics when designing site-specific irrigation strategies.

Irrigation strategy analysis further shows that increasing the ratio of surface water reduces streamflow depletion. However, this does not imply lower total water use, it instead reduces the induced portion of streamflow depletion while increasing direct surface water withdrawals. Therefore, sustainable management requires a balanced groundwater-surface water allocation that both maintains aquifer longevity and protects instream flow.

Marginal analysis reveals that stream-induced water provides limited economic benefit.

The marginal net benefit of depletion remains negative across all scenarios, indicating that
the economic gains from additional irrigation are outweighed by the associated hydrologic

costs (Figure 11). This shows the inefficiency of relying on streamflow depletion to sustain irrigation, even when it buffers groundwater drawdown. From a broader perspective, these findings emphasize the need to protect streamflow, prioritize high-value water uses, and integrate ecological and economic objectives in allocation decisions. In regions with interconnected groundwater-surface water systems, such as the SRB, effective management must recognize the multifaceted trade-offs between farm-level returns and long-term hydrologic sustainability.

Beyond economic trade-offs, streamflow sustains ecosystem services, including aquatic habitat, biodiversity, and water quality regulation. These services, though not quantified in this study, represent significant environmental and social benefits that are vulnerable to groundwater-driven streamflow depletion. A more integrated approach to water management should account for these non-market values, especially as climate variability continues to affect the reliability of both surface and groundwater resources. Incorporating ecological considerations alongside economic assessments is essential for long-term, sustainable land and water use planning.

6 Conclusion

This study integrates analytical methods for quantifying streamflow depletion into a hydro-economic model to examine how groundwater pumping, groundwater-surface water interaction, and boundary conditions jointly shape hydrologic and economic outcomes. Results show that wells located near streams experience faster and more consistent depletion, with water derived from stream through groundwater pumping contributing significantly to irrigated land values. In contrast, wells farther from the stream rely primarily on aquifer storage, leading to delayed depletion and making groundwater the dominant source of economic return. These spatial contrasts show the need to consider well placement and water

source contributions when designing site-specific irrigation strategies. The marginal value analysis further reveals that streamflow depletion provides limited economic gain, emphasizing the trade-offs between short-term profitability and long-term sustainability. Together, these insights highlight the importance of integrating hydrologic connectivity, spatial variability, and economic efficiency into irrigation planning to support sustainable and informed groundwater-surface water management.

7 Author Contributions

B.T.: Conceptualization, Methodology, Data curation, Software, Validation, Visualization, Writing – original draft, Writing – review and editing. A.B.: Conceptualization, Methodology, Validation, Supervision, Writing – review and editing, Project administration, Funding acquisition. M.I.: Validation, Writing – review and editing.

8 Funding Sources

This work was supported by a University of Waterloo Water Institute Seed Grant; University of Waterloo Trailblazer Award; and the Natural Sciences and Engineering Research Council of Canada [Discovery Grant].

References

- AFCC (2013). AAFC Watershed Project. https://open.canada.ca/data/en/dataset/c20d97e7-60d8-4df8-8611-4d499a796493. Accessed: 2024-10-01.
- Ahlfeld, D. P., Schneider, J. C., and Spalding, C. P. (2016). Effects of nonlinear model response on allocation of streamflow depletion: Exemplified by the case of beaver creek, usa. *Hydrogeology Journal*, 24(7):1835–1845.
- Allen, R. G., Pereira, L. S., Raes, D., Smith, M., et al. (1998). Crop evapotranspiration-guidelines for computing crop water requirements-fao irrigation and drainage paper 56. *Fao*, *Rome*, 300(9):D05109.
- Aquanty (n.d.). Hydrogeosphere: Integrated surface and subsurface modelling. https://www.aquanty.com/hydrogeosphere. Accessed: 2024-12-01.
- Axelson, J. N. (2007). Historical streamflow variability in the South Saskatchewan River Basin inferred from a network of tree-ring chronologies. Faculty of Graduate Studies and Research, University of Regina.
- Barlow, P. M. and Leake, S. A. (2012). Streamflow depletion by wells—understanding and managing the effects of groundwater pumping on streamflow. Technical report, US Geological Survey.
- Bonsal, B. R., Aider, R., Gachon, P., and Lapp, S. (2013). An assessment of canadian prairie drought: past, present, and future. *Climate Dynamics*, 41(2):501–516.
- Brookfield, A. (2016). Minimum saturated thickness calculator. Kansas Geological Survey Open-File Report, 3.
- Chen, H., Fan, L., Li, Q., Wang, Y., Liu, D., and Zhao, F. (2025). Future climate change exacerbates streamflow depletion in the wei river basin, china. *Journal of Hydrology*, page 134146.
- Comeau, L. E., Pietroniro, A., and Demuth, M. N. (2009). Glacier contribution to the north and south saskatchewan rivers. *Hydrological Processes: An International Journal*, 23(18):2640–2653.
- Cooper Jr, H. and Jacob, C. E. (1946). A generalized graphical method for evaluating formation constants and summarizing well-field history. *Eos, Transactions American Geophysical Union*, 27(4):526–534.
- Cummings, D. I., Russell, H. A., and Sharpe, D. R. (2012). Buried-valley aquifers in the canadian prairies: geology, hydrogeology, and origin. *Canadian Journal of Earth Sciences*, 49(9):987–1004.

- Danielescu, S., Barbecot, F., and Morand, V. (2021). Groundwater contributions to surface water in the assiniboine delta aquifer (ada): A water quantity and quality perspective. *Journal of Great Lakes Research*, 47(3):788–797.
- DHI Group (n.d.). Mike she: Integrated hydrological modelling. https://www.dhigroup.com/technologies/mikepoweredbydhi/mike-she. Accessed: 2024-12-01.
- Diersch, H.-J. G. (2013). FEFLOW: finite element modeling of flow, mass and heat transport in porous and fractured media. Springer Science & Business Media.
- Ferris, J. G., Knowles, D. B., and Brown, R. H. (1962). Theory of aquifer tests. US Government Printing Office.
- Foglia, L., McNally, A., and Harter, T. (2013). Coupling a spatiotemporally distributed soil water budget with stream-depletion functions to inform stakeholder-driven management of groundwater-dependent ecosystems. *Water Resources Research*, 49(11):7292–7310.
- Fróna, D., Szenderák, J., and Harangi-Rákos, M. (2019). The challenge of feeding the world. Sustainability, 11(20):5816.
- GIN (2021). Groundwater Information Network: Buried Valleys Aquifer System. https://gin.gw-info.net/service/api_ngwds:gin2/en/data/standard.hydrogeologicunit.html?id=216. Accessed: 2024-10-01.
- Glover, R. E. and Balmer, G. G. (1954). River depletion resulting from pumping a well near a river. Eos, Transactions American Geophysical Union, 35(3):468–470.
- Gober, P. and Wheater, H. (2014). Socio-hydrology and the science–policy interface: a case study of the saskatchewan river basin. *Hydrology and Earth System Sciences*, 18(4):1413–1422.
- Hamdi, M. and Goïta, K. (2023). Analysis of groundwater depletion in the saskatchewan river basin in canada from coupled swat-modflow and satellite gravimetry. *Hydrology*, 10(9):188.
- Hemathilake, D. and Gunathilake, D. (2022). Agricultural productivity and food supply to meet increased demands. In *Future foods*, pages 539–553. Elsevier.
- Huang, C.-S., Yang, T., and Yeh, H.-D. (2018). Review of analytical models to stream depletion induced by pumping: Guide to model selection. *Journal of Hydrology*, 561:277–285.
- Huggins, X., Gleeson, T., Eckstrand, H., and Kerr, B. (2018). Streamflow depletion modeling: Methods for an adaptable and conjunctive water management decision support tool. JAWRA Journal of the American Water Resources Association, 54(5):1024–1038.
- Hunt, B. (1999). Unsteady stream depletion from ground water pumping. Groundwater, 37(1):98-102.

- Keshavarz, K. et al. (2021). Vulnerability of transboundary river basins in a changing climate: a case study of the Saskatchewan River Basin. PhD thesis, University of Saskatchewan.
- Kienzle, S. W., Nemeth, M. W., Byrne, J. M., and MacDonald, R. J. (2012). Simulating the hydrological impacts of climate change in the upper north saskatchewan river basin, alberta, canada. *Journal of hydrology*, 412:76–89.
- Klocke, N. L. (2011). Development of crop production functions for irrigation in north central kansas.
- Kustu, M. D., Fan, Y., and Robock, A. (2010). Large-scale water cycle perturbation due to irrigation pumping in the us high plains: A synthesis of observed streamflow changes. *Journal of Hydrology*, 390(3-4):222–244.
- Lapides, D. A., Maitland, B. M., Zipper, S. C., Latzka, A. W., Pruitt, A., and Greve, R. (2022). Advancing environmental flows approaches to streamflow depletion management. Journal of Hydrology, 607:127447.
- Lucas, M. C., Kublik, N., Rodrigues, D. B., Meira Neto, A. A., Almagro, A., Melo, D. d. C., Zipper, S. C., and Oliveira, P. T. S. (2021). Significant baseflow reduction in the sao francisco river basin. *Water*, 13(1):2.
- Mancosu, N., Snyder, R. L., Kyriakakis, G., and Spano, D. (2015). Water scarcity and future challenges for food production. *Water*, 7(3):975–992.
- Marshall, S. J., White, E. C., Demuth, M. N., Bolch, T., Wheate, R., Menounos, B., Beedle, M. J., and Shea, J. M. (2011). Glacier water resources on the eastern slopes of the canadian rocky mountains. *Canadian Water Resources Journal*, 36(2):109–134.
- Martin, D. L., Supalla, R. J., Thompson, C. L., McMullen, B. P., Hergert, G. W., and Burgener, P. A. (2010). Advances in deficit irrigation management. In 5th National Decennial Irrigation Conference Proceedings, 5-8 December 2010, Phoenix Convention Center, Phoenix, Arizona USA, page 1. American Society of Agricultural and Biological Engineers.
- Moore, R., Fleming, S., Menounos, B., Wheate, R., Fountain, A., Stahl, K., Holm, K., and Jakob, M. (2009). Glacier change in western north america: influences on hydrology, geomorphic hazards and water quality. *Hydrological Processes: An International Journal*, 23(1):42–61.
- Palmer, M. A., Lettenmaier, D. P., Poff, N. L., Postel, S. L., Richter, B., and Warner, R. (2009). Climate change and river ecosystems: protection and adaptation options. *Environmental management*, 44:1053–1068.
- ParFlow (2023). Parflow: An open-source, parallel, integrated hydrologic model. https://parflow.org/. Accessed: 2024-12-01.

- Pomeroy, J., de Boer, D., and Martz, L. W. (2005). Hydrology and water resources of saskatchewan. Technical report, Centre for Hydrology, University Saskatchewan, Saskatchewan.
- Richardson, C. W. (1981). Stochastic simulation of daily precipitation, temperature, and solar radiation. *Water resources research*, 17(1):182–190.
- Rockafellar, R. T. and Uryasev, S. (2002). Conditional value-at-risk for general loss distributions. *Journal of banking & finance*, 26(7):1443–1471.
- Rockafellar, R. T., Uryasev, S., et al. (2000). Optimization of conditional value-at-risk. Journal of risk, 2:21–42.
- Samarawickrema, A. and Kulshreshtha, S. (2009). Marginal value of irrigation water use in the south saskatchewan river basin, canada. *Great Plains Research*, pages 73–88.
- Sarykalin, S., Serraino, G., and Uryasev, S. (2008). Value-at-risk vs. conditional value-at-risk in risk management and optimization. In *State-of-the-art decision-making tools in the information-intensive age*, pages 270–294. Informs.
- Tanzeeba, S. and Gan, T. Y. (2012). Potential impact of climate change on the water availability of south saskatchewan river basin. *Climatic Change*, 112:355–386.
- Tian, B., Brookfield, A., and Insley, M. (2025a). Development of a coupled hydro-economic model to support groundwater irrigation decisions. *EarthArXiv*. Preprint.
- Tian, B., Brookfield, A., Insley, M., and Rudolph, D. (2025b). Sustainable groundwater decisions: Hydro-economic model applications to irrigation in contrasting environmental conditions. *EarthArXiv*. Preprint.
- U.S. Geological Survey (2013). Strmdepl08—an extended version of strmdepl with additional analytical solutions to calculate streamflow depletion by nearby pumping wells. https://mi.water.usgs.gov/software/groundwater/CalculateWell/index.html. Accessed: December 1, 2024.
- U.S. Geological Survey (2022a). Modflow and related programs. https://www.usgs.gov/mission-areas/water-resources/science/modflow-and-related-programs. Accessed: December 1, 2024.
- U.S. Geological Survey (2022b). Modflow one-water hydrologic flow model (mf-owhm). https://www.usgs.gov/software/modflow-one-water-hydrologic-flow-model-mf-owhm. Accessed: December 1, 2024.
- USGS (2023). Specific yield, High Plains aquifer [Data set]. U.S. Geological Survey. https://doi.org/10.5066/P9XWB5JH. Accessed: 2024-10-01.

- Zare, M., Azam, S., Sauchyn, D., and Basu, S. (2023). Assessment of meteorological and agricultural drought indices under climate change scenarios in the south saskatchewan river basin, canada. *Sustainability*, 15(7):5907.
- Zipper, S. C., Farmer, W. H., Brookfield, A., Ajami, H., Reeves, H. W., Wardropper, C., Hammond, J. C., Gleeson, T., and Deines, J. M. (2022). Quantifying streamflow depletion from groundwater pumping: a practical review of past and emerging approaches for water management. *JAWRA Journal of the American Water Resources Association*, 58(2):289–312.
- Zipper, S. C., Gleeson, T., Kerr, B., Howard, J. K., Rohde, M. M., Carah, J., and Zimmerman, J. (2019). Rapid and accurate estimates of streamflow depletion caused by groundwater pumping using analytical depletion functions. *Water Resources Research*, 55(7):5807–5829.

A Validation

We use the USGS online streamflow depletion calculator STRMDEPL08 to validate our streamflow depletion model (U.S. Geological Survey, 2013). After unit conversions, the input parameters are shown in Figure A1. The calculator output is 0.1334 cubic feet per second, or approximately 391.93 m³/day, closely matching our model result of 392.07 m³/day.



Figure A1: Screenshot of STRMDEPL08 input values.

B Parameter Sensitivity

This paper uses the Morris method to assess parameter sensitivity, which tests one factor at a time. Figure B1 presents the sensitivity analysis results for all parameters in Glover's and Hunt's methods. The findings indicate that higher hydraulic conductivity (in both the aquifer and streambed), a thicker aquifer, and a wider river increase streamflow depletion. In contrast, larger storage coefficient, greater distance from the stream, or a thicker streambed reduce depletion (Barlow and Leake, 2012).

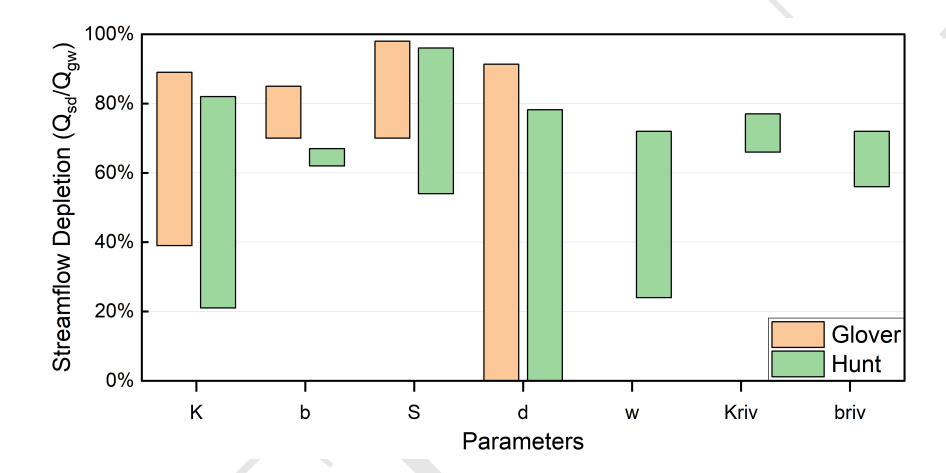


Figure B1: Parameter sensitivity of Glover's and Hunt's methods.

Figure B2 illustrates key patterns in streamflow depletion under different well distances and pumping rates. As expected, wells closer to the stream cause faster and more depletion, while distant wells show delayed and decreased impacts. Seasonal pumping creates a lag between withdrawal and streamflow response, which gradually stabilizes over time. Glover's method consistently produces higher depletion compared to Hunt's, due to its assumption of no streambed resistance.

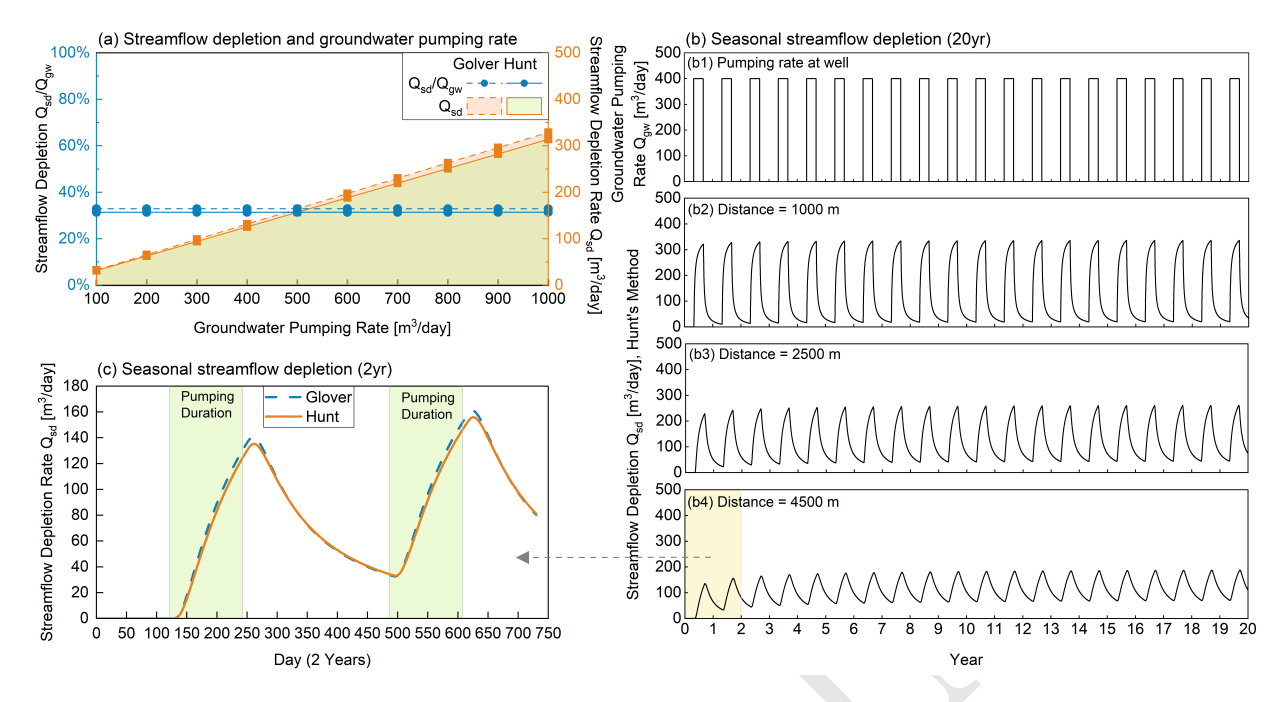


Figure B2: Basic scenarios of confined aquifers: (a) streamflow depletion and pumping rate; (b) 20 years' seasonal streamflow depletion; (c) 2 years' seasonal streamflow depletion.

This model can also be applied to unconfined aquifers. We use a hypothetical aquifer with a higher specific yield (0.2) instead of the storage coefficient (0.0001) used for confined aquifers (GIN, 2021; USGS, 2023). As shown in Figure B3a, the unconfined aquifer has an obvious delayed response in streamflow depletion. In Figure B3b and c, we plot the maximum depletion for each year. The confined aquifer shows high depletion rates, increasing from ~88% to ~91% over time and then stabilizing. In contrast, the unconfined aquifer reaches only ~28% depletion, which gradually declines due to decreasing aquifer thickness.

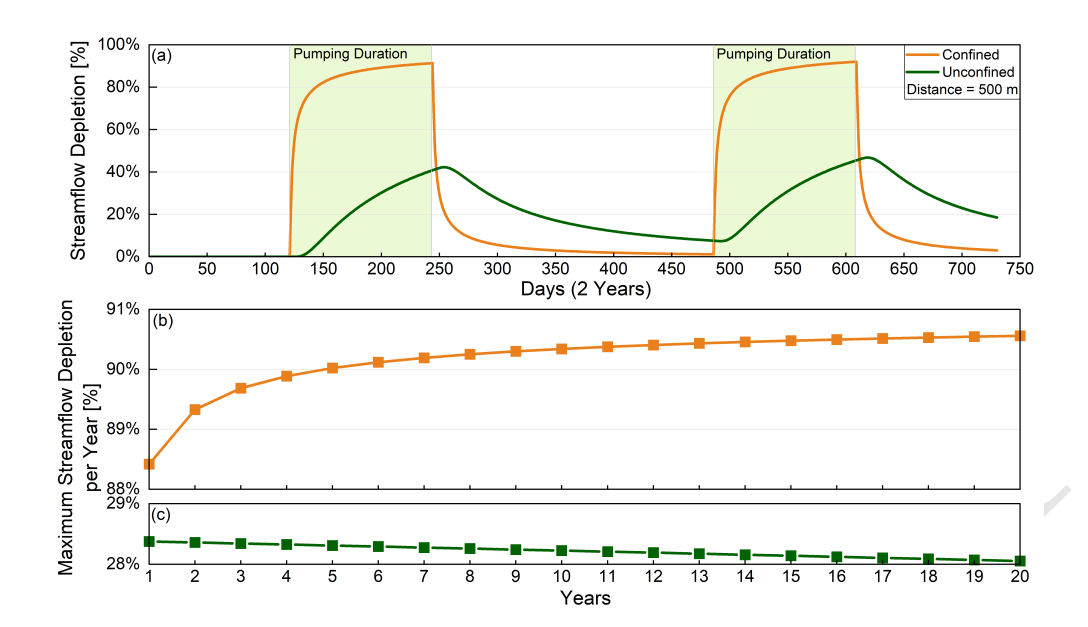


Figure B3: Comparison of streamflow depletion between confined and unconfined aquifers, Hunt's method: (a) seasonal depletion over 2 years; (b) and (c) maximum seasonal depletion over 20 years.